Bone & Joint Research

Supplementary Material

10.1302/2046-3758.1012.BJR-2021-0288.R2

Table i. Characteristics of the RCT studies included in the systematic review.

Study	Country	Objective	Intervention	Sample size, n (male/female)	Mean age, yrs (SD)	Clinical outcome	Follow-up outcome	Complications	Key findings
Shuang et al, 2016	China	Distal intercondylar humeral fractures	A: 3D-printed plates **(Format:** Unite Boolean calculation **3D printer:** SRP400B, Huasen 3D Printing Research, Changzhou, China) B: conventional plates	Total n = 13 (10/3) A: n = 6 (4/2) B: n = 7 (6/1)	A: 46.2 (11.6) B: 40.3 (10.9)	**Operating time (mins):** A (70.6 (SD 12.1)), B (92.3 (SD 17.4)), p = 0.026	**Follow-up period (mths):** 10.6 **ROM of elbow:** **Flexion/extension (°):** A (98 (SD 27)), B (93 (SD 24)), p = 0.730 **Pronation/supination (°):** A (160 (SD 17)), B (167 (SD 21)), p = 0.528 **MEPS (point):** A (85 (SD 9)), B (79 (SD 13)), p = 0.394 **Rate of patients with excellent or good elbow function (%):** A (83.1), B (71.4)	One patient in the conventional group experienced intraoperative traction injury of theulnar nerve. No wound infectionsor other complications were observed	3D method is both safe and effective for the treatment of adults with intercondylar humeral fractures and has a significantly shorter operative time comparedto conventional plates
Zheng et al, 2018	China	Pilon fracture	A: 3D printing group **(Format:** STL **3D printer:** 3D ORTHO Waston Med,Inc., Changzhou, Jiangsu, China) B: conventional group	Total n = 93 (66/27) A: n = 45 (35/10) B: n = 48 (31/17)	A: 41.2 (9.3) B: 42.5 (9.0)	**Operating time (mins):** A (74.1 (SD 8.2)), B (90.2 (SD 10.9)), p < 0.001 **Blood loss (ml):** A (117.1 (SD 20.7)),B (159.8 (SD 26.5)), p < 0.001 **Intraoperative fluoroscopy(times):** A (7.6 (SD 2.2)), B (11.0 (SD 2.9)), p < 0.001 **Rate of anatomical reduction (%):** A (91.1), B (75), p = 0.040 **Fracture union time (mths):** A (5.0 (SD 1.1)), B (5.3 (SD	**Follow-up period (mths):** A (20.5 (SD 3.7)), B (19.9 (SD 3.3)) **ROM of ankle:** **Ankle dorsiflexion (°):** A (15.1 (SD 4.8)),B (14.2 (SD 5.0)), p = 0.409 **Ankle plantar flexion (°):** A (27.4 (SD 8.5)), B (25.9 (SD 8.7)), p = 0.394 **VAS:** A (2.6 (SD 0.9)), B (2.9 (SD 1.2)), p = 0.218 **AOFAS score:** A (87.4 (SD 8.7)), B (84.7 (SD 9.0)), p = 0.149	**Total complication rate:** A:15.6% (7/45) B: 20.8% (10/48),P=0.510	3D printing technology is both safe and effectivefor the treatment of adults with Pilon fractures. Two groups did not differ significantly in functional outcome at the last follow-up period

						1.2)), p = 0.314 **Questionnaire:** Overall satisfaction with the 3D printing model for doctors: 9.0 (SD 1.1)	**Rate of excellent and good outcome in AOFAS (%):** A (93.3), B (77.1)		
Chen et al, 2019	China	AO type C fractures of the distal radius	A: 3D model of distal radius fracture **(Format:** STL **3D printer**: 3D ORTHO; Waston MedInc., Changzhou, Jiangsu, China) **Printing materials:** Polylactic acid B: routine treatment	Total n = 48 (31/17) A; n = 23 (14/9) B: n = 25 (17/8)	A: 38.7 (13.6) B: 40.7 (11.4)	**Operating time (mins):** A (66.5 (SD 5.3)), B (75.4 (SD 6.0)),p < 0.001 **Blood loss volume (ml):** A(41.1 (SD 7.5)), B (54.2 (SD 7.9)), p < 0.001 **Intraoperative fluoroscopy (times):** A (4.4 (SD 1.4)), B (5.6 (SD 1.6)), p = 0.011 **Questionnaire:** **Patients:** 'How much do youknow about your fracture situation' (p = 0.000) & 'How much do you know about your surgical plan' (p = 0.001) **Surgeons:** 'Usefulness of the 3D prototype for communication with patients': (9.1 (SD 0.8)) & 'Overall usefulness of 3D printing models': (6.7 (SD 1.4))	**Follow–up period (mths):** A: 13.0 (SD 0.7) B: 13.1 (SD 0.7) **ROM of wrist:** **extension (°)**: A (4.1 (SD 3.5)), B (3.8 (SD 3.1)), p = 0.765 **Flexion (°):** A (3.1 (SD 2.7)), B (3.6 (SD 2.7)), p = 0.511 **Pronation (°):** A (5.1 (SD 3.2)), B (4.5 (SD 3.7)), p = 0.548 **Supination (°)**: A (4.4 (SD 3.3)), B (4.9 (SD 3.3)), p = 0.613 **Ulnar deviation (°)**: A (20.9 (SD 1.7)), B (20.4 (SD 1.5)), p = 0.309 **Palmar tilt (°)**: A (12.2 (SD 1.5)), B (12.7 (SD 1.9)), p = 0.359 **Radial styloid process (mm)**: A (12.6 (SD 1.9)), B (12.6 (SD 1.8)), p = 0.987 **Gartland–Werley scores:** A (75.7 (SD 15.5)), B (74.8 (SD 16.6)), p = 0.211	N/A	3D printing models effectively help the doctors plan and perform the operation and provide more effective communication between doctors and patients. But cannot improve postoperative function compared withroutine treatment

Huang et al, 2020	China	Both-column acetabular fractures	A: 3D printing group (**Format**: STL **3D printer** Prismlab Rapid400; Prismlab, Shanghai, China) B: conventional group	Total n = 40 (26/14) A: n = 20 (12/8) B: n = 20 (14/6)	A: 43.4 (11.6) B: 37.4 (12.7)	**Operating time (mins):** A (130.8 (SD 29.2)), B (206.3 (SD 34.6)), p < 0.001 **Instrumentation time (mins):** A (32.1 (SD 9.5)), B (57.9 (SD 15.1)), p < 0.001 **Blood loss (ml):** A (500 [400, 800]), B (1,050 [950, 1,200]), p < 0.001 **Blood transfusion (ml):** A: 0 (0, 400), B: 800 (450, 950), p < 0.001 **Intraoperative fluoroscopy (times):** A (4.2 (SD 1.8)), B (7.7 (SD 2.6)), p < 0.001 **Time of bone union (wks):** A (14.48 (SD 1.52)), B (15.85 (SD 1.56)), p = 0.007 **Number of the approach:** A (35%), B (85%), p < 0.05	**Follow-up period (mths):** A: 40.0 (SD 14.5) B: 45.2 (SD 15.2) **Good reduction rate (%):** A (80), B (30), p < 0.05 **Hip joint function (excellent/good rate) (%):** A (75), B (30), p < 0.05	**Complication rate**:(yes/total): A: 5% (1/20) B: 25% (5/20) p = 0.182	3D method can shorten the operation and instrumentation time, reduce blood loss, blood transfusion, and the time of intraoperative fluoroscopy; 3D printing is a more effective method than the conventional method to treat both-column acetabular fractures
You et al,2016	China	Complicated proximal humeral fractures (PHF)	A: 3D printing (**Format:** N/A **Rapid prototyping equipment**: 3D System Project 660Pro) B: thin-layer CT scan	Total n = 66 (27/39) A: n = 34 (15/19) B: n = 32 (12/20)	A: 66.09 (4.09) B: 66.28 (4.10)	**Duration of surgery (mins):** A (77.65 (SD 8.09)), B (92.03 (SD 10.31)), p < 0.05 **Blood loss volume (ml):** A (235.29 (SD 63.40)), B (281.25 (SD 57.85)), p < 0.05 **No. of fluoroscopy (times):** A (7.12 (SD 1.57)), B (10.59 (SD 1.36)), p < 0.05 **Time to fracture union (wks):** A (8.36 (SD 1.00)), B (8.50 (SD 1.22)), p > 0.05	**Follow-up period (mths):** A: 22.38 (SD 4.57) B: 22.19 (SD 4.91)	N/A	3D group had significantly smaller number of fluoroscopies, duration time of surgery and intraoperative blood loss volume, and reduce the potential injury fromsurgery and anaesthesia than the control group. 3D printing has shown great clinical feasibility of the treatment of complicated PHFs

Kong et al, 2020	China	Intra-articular DRFs	A: 3D model group (**Format:** STL) B: routine group	Total n = 32 (19/13) A: n = 16 (10/6) B: n = 16 (9/7)	A: 41.1 (6.4) B: 42.8 (5.1)	**Operating time (mins):** A (51.4 (SD 6.8)), B (63.5 (SD 5.9)), p < 0.001 **Amount of intraoperative bleeding (ml):** A (52.3 (SD 9.9)), B (74.2 (SD 10.3)), p < 0.001 **Intraoperative fluoroscopy (times):** A (4.2 (SD 1.3)), B (5.6 (SD 1.1)), p = 0.002	**Follow-up period (mths):** 6 **ROM:** **Flexion (°):** A (69.3 (SD 5.5)), B (68.4 (SD 7.2)), p = 0.70 **Extension (°):** A (61.2 (SD 9.8)), B (62.1 (SD 11.1)), p = 0.81 **Radial deviation (°):** A (24.8 (SD 5.1)), B (23.2 (SD 4.9)), p = 0.38 **Ulnar deviation (°):** A (22.0 (SD 6.9)), B (19.8 (SD 5.8)), p = 0.35 **Pronation (°):** A (78.0 (SD 14.5)), B (78.4 (SD 13.1)), p = 0.94 **Supination (°):** A (82.0 (SD 12.1)), B (79.9 (SD 16.3)), p = 0.69 **VAS score:** A (0.9 (SD 0.2)), B (0.9 (SD 0.3)), p = 0.91 **DASH score:** A (23.8 (SD 8.1)), B (24.5 (SD 7.0)), p = 0.80	1 patient in B group experienced superficial wound infection, and 1 patient in each group showed loss of reduction, which required no surgical interference. No iatrogenic neurological symptoms or other complications were observed in both groups	3D printing technique help reduce operating time, amount of intraoperative bleeding,and times of intraoperative fluoroscopy. 3D printing technique is safe and effective for surgical treatment of intra-articular DRFs with volar plating and K-wire fixation
Feng et al,2020	China	Cervical spondylotic myelopathy with combination of multilevel developmenta l cervical spine canal stenosis	A: screw insertion assisted by the guidance of 3D printing templates (**Format:** MCS **Printing material:** nylon, Somos Company, USA) B: screw insertion by freehand	Total n = 12 (10/2) A: n = 6 (5/1) B: n = 6 (5/1)	A: 57.67 (11.20) B: 67.17 (5.91)	**Blood lost (ml):** A(300.00 (SD 89.44)), B (350.00 (SD 137.84)), U value = 0.315 **Operating time (mins):** A(171.67 (SD 19.41)), B (175.83 (SD 26.16)), p = 0.760	**Follow-up period:** N/A **JOA score:** A (12.83 (SD 1.17)), B (11.83 (SD 0.98)), p = 0.140 **Our criterion (excellent & good rate) (%):** A (83.3), B (47.2), p = 0.001 **Bayard's criterion (%):** A (88.9), B (61.1), p = 0.014	No neurological complications or infections in both groups	3D printing model preoperatively allow comprehensive visualization of the cervical vertebrae and lateral mass and the individual surgical planning. 3D printing increased the accuracy of cervical lateral mass screw insertion
Du et al, 2013	China	Hip OA	A: patient-specific templates using a rapid prototyping technique (**Format:** STL) B: conventional method	Total n = 34 A: n = 16 (N/A) B: n = 18 (N/A)	N/A	N/A	**Follow-up period:** seven and ten days postoperatively **Radiological evaluation (stem-shaft angle) (°):** A (136.69 (SD 7.70)), B (121.22 (SD 10.69)), p = 0.001	N/A	The 3D template designed and constructed preoperatively can provide precise and dependable location for hip resurfacing femoral components during hip arthroplasty. Also, the 3D method ensured the valgus stem placement necessary for optimal outcomes

Merc et al, 2013	Slovenia	Degenerative disorders resultingin spondylo-lysis+/-listhesis or severe spinal stenosis	A: pedicle screws using drill guide templates (**Format:** STL **3D printing technology:** SLS) B: screws using freehand technique under fluoroscopy supervision	Total n = 19 (9/10) A: n = 9 (4/5) B: n = 10 (5/5)	A: 59 (5) B: 62 (12)	**Operating time (mins):** A (143 (SD 113)), B (176 (SD 90)) **Displacement sagittal:** A (0.3 (SD 3.4)), B (1.5 (SD 3.2)), $p = 0.05$ / A (1.9 (SD 4.1)), B (-1.0 (SD 3.9)), $p = 0.17$ **Deviation sagittal:** A (-1 (SD 5)), B (-6 (SD 8)), $p < 0.001$ / A (2 (SD 10)), B (-12 (SD 8)), $p = 0.01$ **Displacement transversal:** A (-0.7 (SD 1.5)), B (-0.2 (SD 2.6)), $p = 0.28$ / A (-1.4 (SD 2.5)), B (-1.9 (SD 2.1)), $p = 0.72$ **Deviation transversal:** A (-1 (SD 5)), B (0 (SD 11)), $p = 0.71$ / A (-3 (SD 5)), B (-8 (SD 13)), $p = 0.20$ **Screw length violation:** A (14), B (20), $p = 0.21$ / A (3), B (10), $p = 0.36$ **Adopted thoracic screw placement score: Lumbar andsacral level / S1 level** **(Grade 0):** A (50), B (45) / A (6), B (11) **(Grade 1):** A (4), B (8) / A (0), B (3) **(Grade 2):** A (0), B (1) / A (0), B (0) **(Grade 3):** A (0), B (0) / A (0), B (0)	N/A	N/A	The 3D method significantly lowers the incidence of cortex perforation and is therefore potentially applicable in clinical practice, especially in some selected cases. However, the applied 3D method carries a potential for errors during manufacturing and practical usage and therefore still requires further improvements
Zhang et al, 2016	China	Knee OA	A: computer-aided design of navigation template group (NT) (**Format:** STL **3D printer:** SPSS350B solid laser rapid prototyping machine (Shanxi Hengtong Intelligent Machine Co., China) B: CIP	Total n = 40 (26/14) A: n = 20 (12/8) B: n = 20 (14/6)	A: 63.3 (5.1) B: 62.1 (4.9)	**Operating time (mins):** A (46.8 (SD 9.1)), B (57.5 (SD 12.3)), $p = 0.0086$ **Blood loss (ml):** A (463.8 (SD 110.6)), B (478.6 (SD 105.4)), $p = 0.6862$ **Coronal femoral angle:** A (89.4 (SD 1.5)), B (87.3 (SD 3.8)), $p = 0.0435$ **Coronal tibia angle:** A (89.3 (SD 1.4)), B (88.1 (SD 1.9)),$p = 0.0456$ **Posterior tibia slope:** **A** (6.8 (SD 1.6)), B (10.9 (SD 4.6)), $p = 0.0021$ **Sagittal femoral angle:**	**Follow-up period (mths):** 12 **HSS scores:** A (82.9 (SD 16.8)), B (72.8 (SD 10.9)), $p = 0.0472$	No obvious moving, and the postoperative incision healed with no deep venous thrombosis, vascular or nerve damage, or cardiovascular complications	The navigation template produced through mechanical axis of lower limb may provide a relative accurate and simple method for TKA

						A (89.1 (SD 1.8)), B (87.9 (SD 2.8)), p = 0.1445			
Hu et al, 2020	China	Cubitus varus deformity	A: 3D individualized navigation template group (**Format:** Boolean operation **Printing material:** medical polyactic acidmaterial) B: traditional surgery group	Total n = 35 (21/14) A: n = 16 (9/7) B: n = 19 (12/7)	A: 6.86 (1.84) B: 7.79 (2.51)	**Operating time (mins):** A (11.69 (SD 2.21)), B (22.89 (SD 3.94)), p < 0.001	**Follow-up period (mths):** 6 to 12 **Average differences in postoperative carrying angles between affected and healthy sides (°):** A (1.13 (SD 1.20)). B (4.21 (SD 2.27)), p < 0.001 **Max. extension angle of elbow joint mobility (°):** A (1.00 (SD 6.24)), B (2.00 (SD 6.51)), p = 0.648 **Max. flexion angle of elbow joint mobility (°):** A (126.3 (SD 5.33)), B (126.8 (SD 5.08)), p = 0.789 **Bellemore criteria:** p = 0.101	No complications, such as incision infection, non union, neurovascular injuries, pin track infection, and loss of reduction, occurred in both groups	This 3D template can simplify the surgical procedure, reduce the operating time, improve the surgical accuracy, and shorten the learning curve of new clinicians. However, elbow joint function did not significantly differ between the two groups
Sun et al, 2020	China	Advanced OA of the knee	A: patient-specific instrumentation group (**Format:** STL **Laser rapid prototyping printer:** UP BOX,Tiertime, China **Printing material:** polylactic acid) B: conventional TKA	Total n = 80 (15/65) A: n = 40 (8/32) B: n = 40 (7/33)	A: 68.7 (9.1) B: 67.6 (8.4)	**Operating time (mins):** A(87.3 (SD 3.5)), B (73.6 (SD 4.4)), p < 0.001 **Drainage volume (ml):** A (258.7 (SD 11.8)), B (305.6 (SD 10.8)), p < 0.001 **Duration of drainage (hrs):** A (24.5 (SD 3.8)), B (23.6 (SD 4.8)), p > 0.05 **Depth of intramedullary guide (cm):** A (9.4 (SD 2.5)), B (20.4 (SD 3.6)), p < 0.001 **Varus deformity:** A (8.8 (SD 2.5)), B (9.2 (SD 3.6)), p > 0.05	**Follow-up period (mths):** 9.0 (SD 3.9) **ROM:** A (124.2 (SD 14.3)), B (123.4 (SD 12.0)), p > 0.05 **HSS score:** A (87.4 (SD 8.2)), B (86.3 (SD 7.6)), p > 0.05 **AKS score:** A (85.7 (SD 8.7)), B (84.1 (SD 7.2)), p > 0.05 **PFA:** A (0.5 (SD 0.3)), B (3.1 (SD 1.0)), p < 0.001 **HKA:** A (178.6 (SD 0.7)), B (178.8 (SD 0.8)), p > 0.05 **PCA:** A (0.4 (SD 0.2)), B (1.7 (SD 2.0)), p < 0.001	No intraoperative or early postoperative complications occurred in the PSI group and the conventional group	3D method had the advantages of correct alignment, as well as the disadvantages of prolonged operating time and higher cost. The clinical outcomes inthe short term of TKA assisted by 3D printing of PSI was satisfactory in the postoperative follow-up. However, further studies are needed to confirm the long-term clinical effects

Wu et al, 2020	China	CLAI	A: 3D printed template group (**Format:** STL **Printing material:** photosensitive resin material) B: traditional intraoperative fluoroscopy-guided method	Total N = 34 (14/20) A: n = 18 (7/11) B: n = 16 (7/9)	A: 26.5 (7.3) B: 23.6 (5.1)	**Operating time (mins):** A (51.9 (SD 3.6)), B (72.4 (SD 12.6)), p < 0.01 **Intraoperative radiation exposure (times):** A (1.34 (SD 0.6)), B (6.58 (SD 1.7)), p < 0.01	**Follow-up period (month):** A: 23±3.6 B: 25±2.8 **Anterior drawer (stress radiography) (mm):** A (1.9±0.8), B(2.1±0.5), P is NS **Talar tilt test (stress radiography) (degrees):** A (3.2±0.6), B (3.4±0.7), P is NS **AOFAS score:** A (95.2±2.5), B(94.9±2.2), P>0.01 **Karlsson-Peterson score:** A (94.7±3.6), B (93.8±4.1), P>0.01	N/A	The 3D template cohort group have shorter operation duration and fewer radiation exposures, suggest it is abetter alternative for the treatment of CLAI. Besides, no significant differences of the anterior talar displacement and the talar tilt angle between two groups
Yin et al, 2020	China	Scaphoid nonunion without displacement	A: 3D printing guide plate assisted fixation + arthroscopy bone grafting (**Printer:** Objet30 prime, Stratasys, MN, USA with a photopolymer of medical compatibility (MED610, Stratasys, MN, USA) B: fixation with intra-operative fluoroscopy + arthroscopy bonegrafting	Total n = 16 (15/1) A: n = 8 (8/0) B: n = 8 (7/1)	A: 28.0 (6.9) B: 35.0 (10.0)	**Bone operating time (mins):** A (69.4 (SD 15.3)), B (94.1 (SD 18.7)), p = 0.012	**Follow-up period (mths):** 6 **ROM ratio (injured/healthy):** **Flexion-extension:** A (0.78 (SD 0.12)), B (0.71 (SD 0.11)) **Radioulnar deviation:** A (0.68 (SD 0.14)), B (0.67 (SD 0.14)) **Pronation-supination:** A (1.00 (SD 0.12)), B (0.9 (SD 0.05)) **Strength ratio (injured/healthy):Grip strength:** A (0.88 (SD 0.09)), B (0.79 (SD 0.12)) **Pinch strength:** A (0.89 (SD 0.07)), B (0.85 (SD 0.06)) **VAS:** A (0.96 (SD 0.6)), B (1.73 (SD 0.84)) **Modified Mayo scores:** A (84.4 (SD 7.8)), B (72.5 (SD 10)) **PRWE scores:** A (9 (SD 7)), B (14.8 (SD 8.7))	N/A	3D printing is an effective clinical treatment option with a good union rate and wrist function recovery. But there is no statistical difference between 3D printing and conventional group about the changes of ROM ratios, strength ratios, or wrist function scores

Zhang et al, 2020	China	Thoracolumbar fracture	A: porous polyoxymethylene thermoplastic regulator combined with a 3D printed template (**Format:** STL **3D printer**: Pulisheng Electromechanical Technology Co., Ltd., Shanghai, China) **Material:** Photosensitive resin) B: conventional PPSF	Total N = 40 (12/28) A: n = 20 (5/15) B: n = 20 (7/13)	A: 56.57 (5.50) B: 57.33 (4.63)	**No. of pedicles successful pierced at first attempt:** A (10), B (3), p = 0.043 **No. of insertions before reaching the desired position(n):** A (7.83 (SD 1.47)), B (17.50 (SD 1.87)), p < 0.01 **Radiation dosage before reaching the desired position (mSv):** A (0.45 (SD 0.10)), B (1.35 (SD 1.38)), p < 0.01 **Operating time before reaching the desired position (mins):** A (15.17 (SD 2.64)), B (29.50 (SD 2.43)), p < 0.01 **Total operating time (mins):** A (66.67 (SD 6.80)), B (95.50 (SD 7.18)), p < 0.01 **Total radiation dosage of fluoroscopy (mSv):** A (2.75 (SD 0.48)), B (4.82 (SD 0.75)), p < 0.01 **Intraoperative blood loss (ml):** A (86.50 (SD 5.32)), B (127.33 (SD 5.05)), p < 0.01	**Follow-up period:** at one day before surgery, at day 1, day 7, month 1, and month 3 after surgery **KA:** A (5.83 (SD 0.75)), B (6.83 (SD 1.47)), p = 0.169 **No. of vertebral pedicles damaged:** A (1), B (8), p = 0.029 **VAS Day 1:** A (3.17 (SD 0.75)), B (6.50 (SD 0.55)), p < 0.01 **VAS Month 3:** A (1.33 (SD 0.52)), B (1.50 (SD 0.55)), p = 0.60 **ODI Day 1:** A (36.50 (SD 1.05)), B (43.67 (SD 1.97)), p < 0.01 **ODI Month 3:** A (14.17 (SD 0.76)), B (16.17 (SD 0.98)), p = 0.627	No significant nerve and vascular damage and no symptoms of nerve injury (p < 0.05)	3D group may improvethe success of pedicle insertion in patients undergoing PPSF. In short term, 3D printing group reduced postoperative pain, which resulted in more rapid postoperative recovery
Hasan et al, 2020	Sweden	OA Ahlbäck stages IIto IV	A: cementless 3D-printed cruciate-retaining TKA (**Format:** STL **Material:** Tritanium (Stryker, Allendale, New Jersey, USA) B: cemented cruciate-retaining TKA	Total n = 69 (36/33)A: n = 35 (18/17) B: n = 34 (18/16)	A: 65 (5.7) B: 66 (6.3)	**Surgery duration (mins):** A(43 (SD 6.0)), B (45 (SD 4.6))	**Follow-up period:** at 3 mths, 1 yr, and 2 yrs follow-up **KSS-Knee score:** A (33 (SD 9.2)), B (30 (SD 8.9)), p = 0.117 **KSS-Function score:** A (61 (SD 5.9)), B (61 (SD 4.4)), p = 0.459 **KOOS Symptoms:** p = 0.806 **Pain:** p = 0.740 **Activities of daily living:** p = 0.676 **Sports and recreation:** p = 0.546 **Quality of life:** p = 0.725 **FJS:** p = 0.922 **Mean migration:** p = 0.497 **MTPM at three, 12, and 24 mths (mm):** A (0.52, 0.62, and 0.64), B (0.33, 0.42, and 0.47), p = 0.003	In the 3D group, oneimplant was revised due to pain and progressive migration, and one patient had a liner-exchange due to a deep infection	3D group of TKA migrate more than the conventional group in the first 2-year period. This difference was mainly due to a higher initial migration of the 3D group in the first 3 postoperative months. Also, a longer follow-upis required to study whether the biological fixation of the cementless implants will result in an increased long-term survivorship

Wei et al, 2020	China	Cervical spondylotic myelopathy	A: AVB fabricated by electron beam melting (**3D printing techniques:** EBM (Arcam AB, Sweden), **Material:** titanium alloy powder (Ti6Al4V, particle size 45 to 100 μm) B: conventional titanium mesh cage	Total n = 40 (25/15) A: n = 20 (14/6) B: n = 20 (11/9)	A: 55.2 (11.4) B: 53.8 (7.8)	N/A	**Follow-up period (mths):** 6 **Rate of fusion (%):** A (100), B (95), p = 0.995 **Loss of height of the fusion segments:** A (1.39 (SD 1.05)), B(2.39 (SD 1.68)), p = 0.015 **Rate of severe subsidence (%):** A (5), B (35), p = 0.018 **Global lordosis (C2–7):** A (17.9 (SD 5.0)), B (20.4 (SD 8.5)), p = 0.136 **JOA scores:** A (16.35 (SD 0.93)), B (15.35 (SD 1.81)), p = 0.019 **Recovery rate (%):** A (80.8 (SD 27.0)), B (69.1 (SD 25.1)), p = 0.081 **SF-36:** A (66.3 (SD 18.2)), B (68.9(SD 13.4)), p = 0.695 **Odom's criteria:** p = 0.716	One patient in B group whose radiological studies showed signs of screw loosening	3D group has decreased loss of the height of the fusion mass and a lower rate for severe implant subsidence. 3D group has comparable clinical outcomes regarding improvement in neurological function and health-related quality of life to conventional group

Yang et al, 2016	China	Trimalleolar fractures	A: 3D printing assisted-design group (**Format:** STL **3D printer:** FlashForge Ltd., ZhengJiang, China). **Printing material:** Polylactic acid (FlashForge Ltd., 1.75 mm in diameter) B: no 3D printing assisted-design group	Total n = 30 (16/14) A: n = 15 (N/A) B: n = 15 (N/A)	36.5	**Operating time (mins):** A (71 (SD 23)), B (98 (SD 20)), p = 0.587 **Intraoperative blood loss (ml):** A (65 (SD 26)), B (90 (SD 38)), p = 0.709 **Overall satisfaction with the 3D prototype (doctors):** 8.8 (SD 0.4) **Usefulness of the 3D prototype for preoperative planning (doctors):** 8.9 (SD 0.7) **Overall satisfaction of the conversation (patients):** 9.3 (SD 0.6)	N/A	N/A	3D printing can reflect the anatomy accurately, and effectively helps the doctors plan the operation and provide more effective communication between doctors and patients
Maini et al, 2018	India	Acetabular fractures	A: virtually pre-contoured 3D printed template (**Format:** STL **Printing material:** polylactic acid B: conventional method of manual contouring	Total n = 25 (23/2) A: n = 12 (11/1) B: n = 13 (12/1)	N/A	**Duration of surgery (mins):** A (111), B (119) **Total blood loss (ml):** A (467), B (525)	**Follow-up period:** N/A **Postoperative reduction on radiographs: (anatomical reduction):** A (5), B (3) **(satisfactory):** A (4), B (5) **(poor):** A (3), B (5) **Postoperative reduction on NCCT (mm):** A (3.76), B (4.09) **Diff. of displacement on preoperative and postoperative NCCT(mm):** A (12.43), B (9.408)	N/A	3D printing technologyreduced duration and invasiveness of surgery and improving the quality of reduction, which improve the outcomes of acetabular fracture surgery

Zheng et al, 2018 (2)	China	Calcaneal fractures	A: 3D-Printing Group (**Format:** STL **3D printer:** 3DORTHOWaston Med Inc. Changzhou, Jiangsu, China) B: conventional group	Total n = 75 (44/31) A: n = 35 (19/16) B: n = 40 (25/15)	A: 44.5 (8.0) B: 46.7 (6.2)	**Operation duration (mins):** A(71.4 (SD 6.8)), B (91.3 (SD 11.2)), p < 0.0001 **Blood loss volume (ml):** A (226.1 (SD 22.6)), B (288.7 (SD 34.8)). p < 0.0001 **Intraoperative fluoroscopy (times):** A (5.6 (SD 1.9)). B (8.6 (SD 2.7)), p < 0.0001 **Fracture union time (mths):** A(3.0 (SD 0.3)), B (3.2 (SD 0.4)), p = 0.232 **Overall satisfaction with the 3D printing model (doctors):** 8.9 (SD 0.9) **(patients):** 9.1 (SD 0.8)	**Follow-up period (mths):** A: 14.9 (SD 1.9) B: 14.7 (SD 2.0) **Radiological outcomes (angle restoration in postoperative andfinal follow up):** **Böhler angle (°):** A (31.7 (SD 5.0)), B (27.5 (SD 4.3)), p = 0.0002 / A (32.5 (SD 4.6)), B (29.7 (SD 5.4)), p = 0.0160 **Gissane angle (°):** A (134.5 (SD 5.8)), B (138.0 (SD 6.6)), p = 0.0183 / A (129.6 (SD 6.0)), B (133.7 (SD 7.0)), p = 0.0085 **Calcaneal width (mm):** A (36.5 (SD 3.0)), B (38.5 (SD 2.8)), p = 0.004 / A (35.1 (SD 4.1)), B (37.1 (SD 3.9)), p = 0.0383 **Calcaneal height (mm):** A (42.3 (SD 3.5)), B (40.4 (SD 2.4)), p = 0.0065 / A (44.6 (SD 2.6)), B (41.9 (SD 2.2)), p < 0.0001 **VAS score:** A (2.6 (SD 0.9)), B (2.8 (SD 1.2)), p = 0.369 **AOFAS score:** A (87.6 (SD 7.6)), B (85.8 (SD 9.0)), p = 0.341 **AOFAS: Rate of excellent and goodoutcome (%):** A (88.6), B (85), p = 0.910	A: 17.1% (6/35) B: 20% (8/40),p = 0.751	Surgery assisted by 3D printing technology can achieve better surgical outcomes and radiological outcomes inthe treatment of calcaneal fractures, suggesting that 3D printing technology is safe and effective for the treatment of calcaneal fractures. Also, 3D printing technology provides better communication between doctors and patients. But two groups did not differ significantly in functional outcome at the last follow-up period
Zheng et al, 2018 (3)	China	Humeral intercondyl arfractures	A: 3D-printing group (**Format:** STL **3D printer:** 3D ORTHO Waston MedInc. Changzhou, Jiangsu, China) B: conventional group	Total n = 91 (49/42) A: n = 43 (24/19) B: n = 48 (25/23)	A: 44.7 (4.8) B: 44.5 (4.5)	**Operation duration (mins):** A(76.6 (SD 7.9)), B (92.0 (SD 10.5)), p < 0.0001 **Blood loss volume (ml):** A (231.1 (SD 18.1)), B (278.6 (SD 23.0)), p < 0.0001 **Intraoperative fluoroscopy (times):** A (5.3 (SD 1.9)), B (8.7 (SD 2.7)), p < 0.0001 **Time to fracture union(mths):** A (3.0 (SD 0.3)), B (3.1 (SD 0.4)), p = 0.1537 **Overall satisfaction with the3D-printing model (doctors/patients):** 8.9 (SD 0.9) / 9.0 (SD 0.9)	**Follow-up period (mths):** A: 15.3 (SD 2.0) B: 15.7 (SD 2.3) **ROM of elbow (°):** **Flexion:** A (115.2 (SD 17.1)), B(112.3 (SD 16.6)), p = 0.416 **Extension:** A (23.8 (SD 8.1)), B (24.8 (SD 7.9)), p = 0.569 **Pronation:** A (80.1 (SD 6.4)), B (80.7 (SD 8.1)), p = 0.690 **Supination:** A (81.3 (SD 7.6)), B (79.8 (SD 7.7)), p = 0.382 **MEPS score:** A (85.2 (SD 9.6)), B (83.1 (SD 10.0)), p = 0.448 **DASH score:** A (21.5 (SD	**Complication rate:** A: 9.3% (4/43), B: 12.5% (6/48) **Wound infections:** A (3), B (4) **Ulnar nerve paraesthesi a:** A (1), B (2)	3D printing technology is safe and effective for the treatment of intercondylar humeral fractures. Also, 3D printing technology provides a better communication between doctors and patients. Yet, the two groups did not differ significantly in elbow function at the last follow-up period

							6.4)), B (22.8 (SD 5.1)), p = 0.279		

AKS, American Knee Society score; AOFAS, The American Orthopedic Foot and Ankle Society score; AVB, artificial vertebral body; CIP, conventional intramedullary positioning group; CLAI, chronic lateral ankle instability; DASH, The Disabilities of the Arm, Shoulder and Hand score; DRF, distal radius fracture; EBM, electronbeam melting; FJS, Forgotten Joint Score; JOA, Japanese Orthopaedic Association; HKA, hip-knee-ankle angle; HSS, Hospital for Special Surgery knee score; KA, kyphotic angle; KSS, Knee Society Score; MCS, Materialise Mimics; MEPS, The Mayo Elbow Performance Score; PCA, posterior condylar angle; PFA, patella transverse axis-femoral transepicondylar axis angle; PPSF, percutaneous pedicle screw fixation; PRWE, Patient-Rated Wrist Evaluation; OA, osteoarthritis; ODI, Oswestry Disability Index; ROM, range of motion; SD, standard deviation; SLS, selective laser sintering; STL, stereolithography; TKA, total knee arthroplasty; VAS, visual analogue scale.

	3D printing			Conventional approach				Std. Mean Difference
Study or Subgroup	**Mean**	**SD**	**Total**	**Mean**	**SD**	**Total**	**Weight**	**IV, Random, 95% CI**
2.1.1 Upper limb								
Chen et al, 2019	66.5	5.4	23	75.4	6	25	5.4%	-1.53 [-2.18, -0.88]
Hu et al, 2020	11.69	2.21	16	22.89	3.94	19	5.0%	-3.35 [-4.41, -2.28]
Kong et al, 2020	51.4	6.8	16	63.5	5.9	16	5.2%	-1.85 [-2.70, -1.01]
Shuang et al, 2016	70.6	12.1	6	92.3	17.4	7	4.7%	-1.33 [-2.58, -0.08]
Yin et al, 2020	69.4	15.3	8	94.1	18.7	8	4.9%	-1.37 [-2.49, -0.25]
You et al, 2016	77.65	8.09	34	92.03	10.31	32	5.5%	-1.54 [-2.09, -0.99]
Zheng et al, 2018 (3)	76.6	7.9	43	92	10.5	48	5.6%	-1.63 [-2.11, -1.15]
Subtotal (95% CI)			**146**			**155**	**36.4%**	**-1.74 [-2.13, -1.35]**
Heterogeneity: $Tau^2 = 0.11$; $Chi^2 = 10.66$, df = 6 (P = 0.10); $I^2 = 44\%$								
Test for overall effect: Z = 8.81 (P < 0.00001)								
2.1.2 Spine								
Feng et al, 2020	171.67	19.41	6	175.83	26.16	6	4.9%	-0.17 [-1.30, 0.97]
Merc et al, 2013	143	113	9	176	90	10	5.2%	-0.31 [-1.22, 0.60]
Zhang et al, 2020	66.67	6.8	20	95.5	7.18	20	4.9%	-4.04 [-5.16, -2.92]
Subtotal (95% CI)			**35**			**36**	**14.9%**	**-1.50 [-3.90, 0.91]**
Heterogeneity: $Tau^2 = 4.22$; $Chi^2 = 31.40$, df = 2 (P < 0.00001); $I^2 = 94\%$								
Test for overall effect: Z = 1.22 (P = 0.22)								
2.1.3 Lower limb/pelvis								
Hasan et al, 2020	43	6	35	45	4.6	34	5.6%	-0.37 [-0.85, 0.11]
Huang et al, 2020	130.8	29.2	20	206.3	34.6	20	5.3%	-2.31 [-3.13, -1.49]
Maini et al, 2018	111.33	38.23	12	118.84	31.1	13	5.3%	-0.21 [-1.00, 0.58]
Sun et al, 2020	87.3	3.5	40	73.6	4.4	40	5.4%	3.41 [2.72, 4.11]
Wu et al, 2020	51.9	3.6	18	72.4	12.6	16	5.2%	-2.22 [-3.10, -1.34]
Yang et al, 2016	71	23	15	98	20	15	5.3%	-1.22 [-2.01, -0.43]
Zhang et al, 2016	46.8	9.1	20	57.5	12.3	20	5.4%	-0.97 [-1.63, -0.31]
Zheng et al, 2018	74.1	8.2	45	90.2	10.9	48	5.6%	-1.65 [-2.12, -1.17]
Zheng et al, 2018 (2)	71.4	6.8	35	91.3	11.2	40	5.5%	-2.09 [-2.66, -1.52]
Subtotal (95% CI)			**240**			**246**	**48.7%**	**-0.84 [-1.93, 0.24]**
Heterogeneity: $Tau^2 = 2.61$; $Chi^2 = 201.86$, df = 8 (P < 0.00001); $I^2 = 96\%$								
Test for overall effect: Z = 1.53 (P = 0.13)								
Total (95% CI)			**421**			**437**	**100.0%**	**-1.28 [-1.92, -0.65]**
Heterogeneity: $Tau^2 = 1.80$; $Chi^2 = 266.73$, df = 18 (P < 0.00001); $I^2 = 93\%$								
Test for overall effect: Z = 3.99 (P < 0.0001)								
Test for subgroup differences: $Chi^2 = 2.36$, df = 2 (P = 0.31), $I^2 = 15.3\%$								

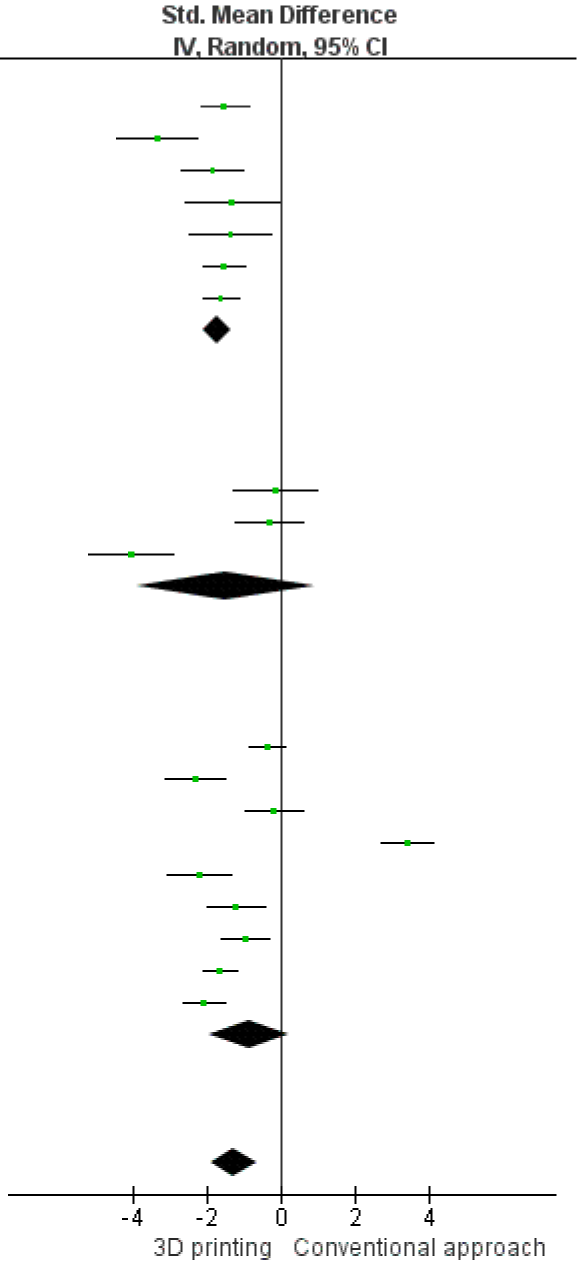

Figure a. The forest plot of subgroup analysis for operating time (mins). CI, confidence interval; IV, inverse variance; SD, standard deviation.

Study or Subgroup	3D printing Mean	3D printing SD	3D printing Total	Conventional approach Mean	Conventional approach SD	Conventional approach Total	Weight	Std. Mean Difference IV, Random, 95% CI
4.1.1 Upper limb								
Chen et al, 2019	41.1	7.5	23	54.2	7.9	25	8.0%	-1.67 [-2.34, -1.01]
Kong et al, 2020	52.3	9.9	16	74.2	10.3	16	7.5%	-2.11 [-3.00, -1.23]
You et al, 2016	235.29	63.4	34	281.25	57.85	32	8.3%	-0.75 [-1.25, -0.25]
Zheng et al, 2018 (3)	231.1	18.1	43	278.6	23	48	8.3%	-2.26 [-2.79, -1.73]
Subtotal (95% CI)			**116**			**121**	**32.1%**	**-1.67 [-2.45, -0.90]**
Heterogeneity: Tau² = 0.51; Chi² = 18.41, df = 3 (P = 0.0004); I² = 84%								
Test for overall effect: Z = 4.26 (P < 0.0001)								
4.1.2 Spine								
Feng et al, 2020	300	89.44	6	350	137.84	6	6.9%	-0.40 [-1.55, 0.75]
Zhang et al, 2020	86.5	5.32	20	127.33	5.05	20	5.1%	-7.72 [-9.60, -5.83]
Subtotal (95% CI)			**26**			**26**	**12.0%**	**-4.02 [-11.19, 3.15]**
Heterogeneity: Tau² = 26.14; Chi² = 42.22, df = 1 (P < 0.00001); I² = 98%								
Test for overall effect: Z = 1.10 (P = 0.27)								
4.1.3 Lower limb/pelvis								
Huang et al, 2020	629.3	377.63	20	1,077.25	188.61	20	7.9%	-1.47 [-2.18, -0.76]
Maini et al, 2018	466.7	123.04	12	525.38	203.15	13	7.7%	-0.33 [-1.13, 0.46]
Sun et al, 2020	258.7	11.8	40	305.6	10.8	40	7.8%	-4.11 [-4.89, -3.32]
Yang et al, 2016	65	26	15	90	38	15	7.9%	-0.75 [-1.49, -0.00]
Zhang et al, 2016	463.8	110.6	20	478.6	105.4	20	8.1%	-0.13 [-0.75, 0.49]
Zheng et al, 2018 (2)	117.1	20.7	45	159.8	26.5	48	8.3%	-1.77 [-2.26, -1.29]
Zheng et al, 2018 (3)	226.1	22.6	35	288.7	34.8	40	8.2%	-2.08 [-2.65, -1.51]
Subtotal (95% CI)			**187**			**196**	**55.9%**	**-1.52 [-2.41, -0.63]**
Heterogeneity: Tau² = 1.32; Chi² = 78.36, df = 6 (P < 0.00001); I² = 92%								
Test for overall effect: Z = 3.35 (P = 0.0008)								
Total (95% CI)			**329**			**343**	**100.0%**	**-1.81 [-2.47, -1.15]**
Heterogeneity: Tau² = 1.29; Chi² = 141.75, df = 12 (P < 0.00001); I² = 92%								
Test for overall effect: Z = 5.40 (P < 0.00001)								
Test for subgroup differences: Chi² = 0.50, df = 2 (P = 0.78), I² = 0%								

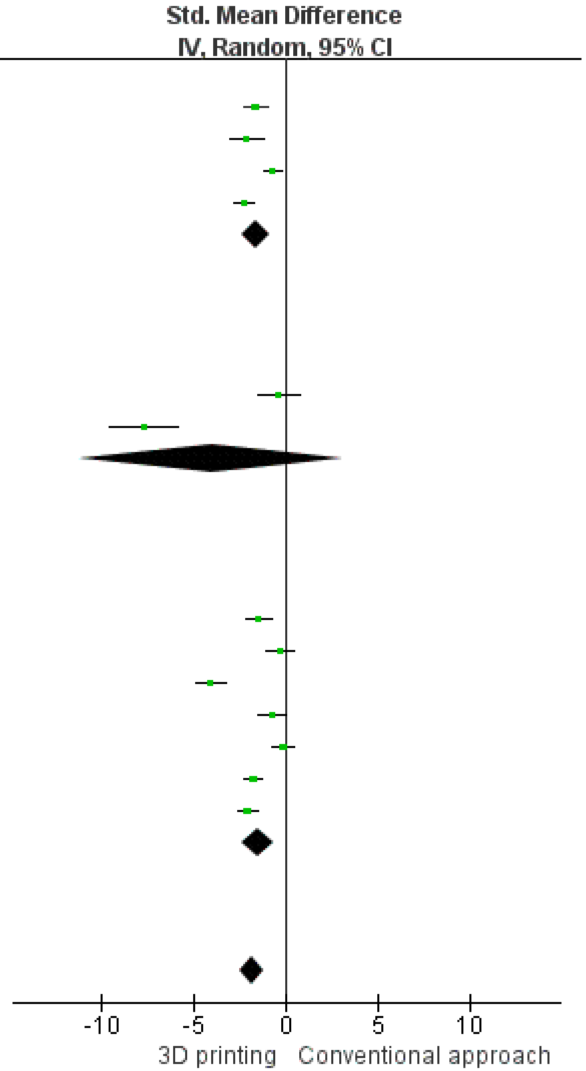

Figure b. The forest plot of subgroup analysis for blood loss (ml). CI, confidence interval; IV, inverse variance; SD, standard deviation.

Study or Subgroup	3D printing Mean	SD	Total	Conventional approach Mean	SD	Total	Weight	Std. Mean Difference IV, Random, 95% CI
6.1.1 Upper Limb								
Chen et al, 2019	4.4	1.4	23	5.6	1.6	25	13.2%	-0.78 [-1.37, -0.19]
Kong et al, 2020	4.2	1.3	16	5.6	1.1	16	11.6%	-1.13 [-1.89, -0.38]
You et al, 2016	7.12	1.57	34	10.59	1.36	32	12.8%	-2.33 [-2.96, -1.70]
Zheng et al, 2018 (3)	5.3	1.9	43	8.7	2.7	48	14.4%	-1.43 [-1.89, -0.97]
Subtotal (95% CI)			**116**			**121**	**51.9%**	**-1.42 [-2.04, -0.80]**
Heterogeneity: Tau² = 0.31; Chi² = 12.97, df = 3 (P = 0.005); I² = 77%								
Test for overall effect: Z = 4.47 (P < 0.00001)								
6.1.2 Lower limb/pelvis								
Huang et al, 2020	4.2	1.8	20	7.7	2.6	20	12.0%	-1.53 [-2.25, -0.82]
Wu et al, 2020	1.34	0.6	18	6.58	1.7	16	7.6%	-4.11 [-5.35, -2.88]
Zheng et al, 2018	7.6	2.2	45	11	2.9	48	14.5%	-1.30 [-1.75, -0.85]
Zheng et al, 2018 (2)	5.6	1.9	35	8.6	2.7	40	14.1%	-1.26 [-1.76, -0.76]
Subtotal (95% CI)			**118**			**124**	**48.1%**	**-1.85 [-2.66, -1.05]**
Heterogeneity: Tau² = 0.53; Chi² = 18.74, df = 3 (P = 0.0003); I² = 84%								
Test for overall effect: Z = 4.53 (P < 0.00001)								
Total (95% CI)			**234**			**245**	**100.0%**	**-1.60 [-2.06, -1.14]**
Heterogeneity: Tau² = 0.33; Chi² = 31.82, df = 7 (P < 0.0001); I² = 78%								
Test for overall effect: Z = 6.82 (P < 0.00001)								
Test for subgroup differences: Chi² = 0.70, df = 1 (P = 0.40), I² = 0%								

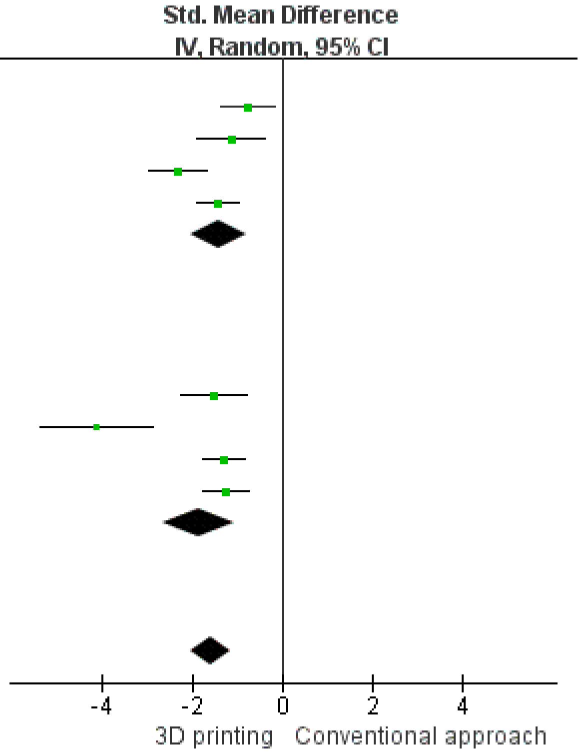

Figure c. The forest plot of subgroup analysis for fluoroscopy times. CI, confidence interval; IV, inverse variance; SD, standard deviation.

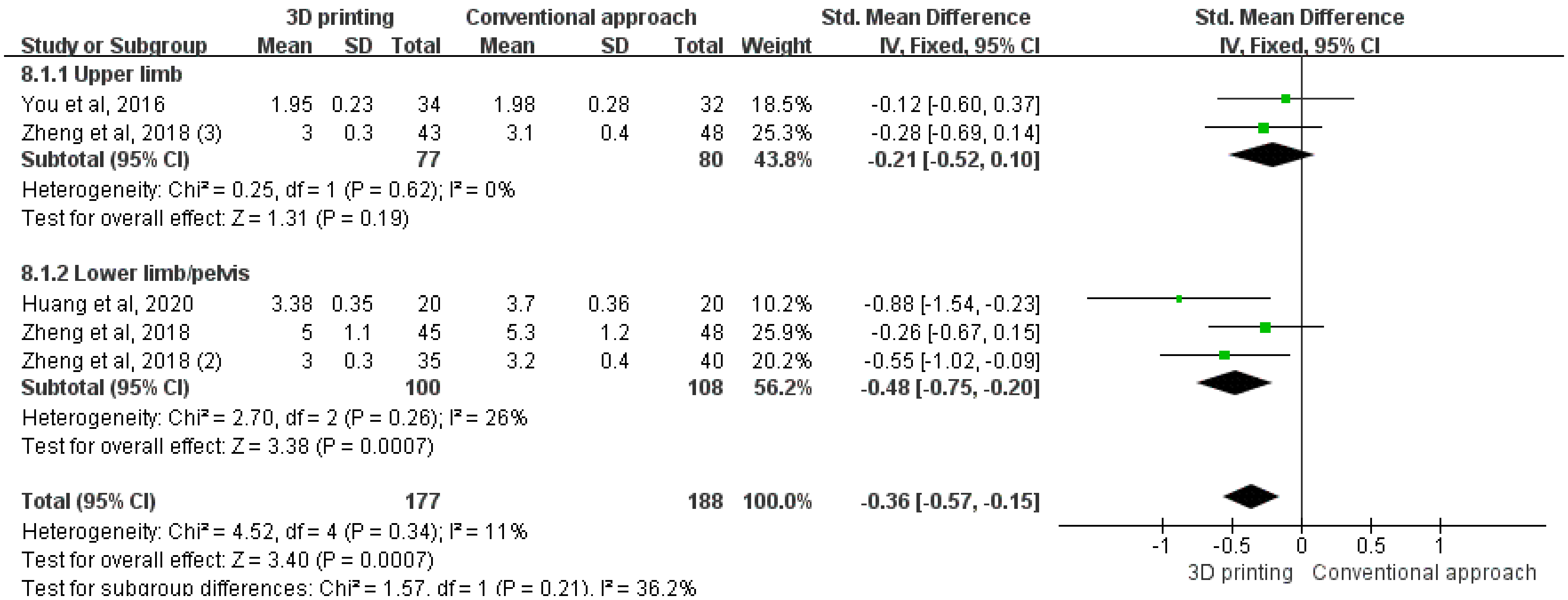

Figure d. The forest plot of subgroup analysis for bone union time (mths). CI, confidence interval; IV, inverse variance; SD, standard deviation.

	3D printing			Conventional approach				Std. Mean Difference
Study or Subgroup	Mean	SD	Total	Mean	SD	Total	Weight	IV, Fixed, 95% CI
12.1.1 Upper limb								
Kong et al, 2020	0.9	0.2	16	0.9	0.3	15	12.4%	0.00 [-0.70, 0.70]
Yin et al, 2020	0.96	0.6	8	1.73	0.84	8	5.5%	-1.00 [-2.06, 0.06]
Subtotal (95% CI)			**24**			**23**	**17.8%**	**-0.31 [-0.89, 0.28]**
Heterogeneity: Chi² = 2.37, df = 1 (P = 0.12); I² = 58%								
Test for overall effect: Z = 1.02 (P = 0.31)								
12.1.2 Spine								
Zhang et al, 2020	1.33	0.52	20	1.5	0.55	20	15.8%	-0.31 [-0.94, 0.31]
Subtotal (95% CI)			**20**			**20**	**15.8%**	**-0.31 [-0.94, 0.31]**
Heterogeneity: Not applicable								
Test for overall effect: Z = 0.98 (P = 0.33)								
12.1.3 Lower limb								
Zheng et al, 2018	2.6	0.9	45	2.9	1.2	48	36.7%	-0.28 [-0.69, 0.13]
Zheng et al, 2018 (2)	2.6	0.9	35	2.8	1.2	40	29.7%	-0.18 [-0.64, 0.27]
Subtotal (95% CI)			**80**			**88**	**66.4%**	**-0.24 [-0.54, 0.07]**
Heterogeneity: Chi² = 0.09, df = 1 (P = 0.76); I² = 0%								
Test for overall effect: Z = 1.53 (P = 0.13)								
Total (95% CI)			**124**			**131**	**100.0%**	**-0.26 [-0.51, -0.01]**
Heterogeneity: Chi² = 2.53, df = 4 (P = 0.64); I² = 0%								
Test for overall effect: Z = 2.07 (P = 0.04)								
Test for subgroup differences: Chi² = 0.07, df = 2 (P = 0.96), I² = 0%								

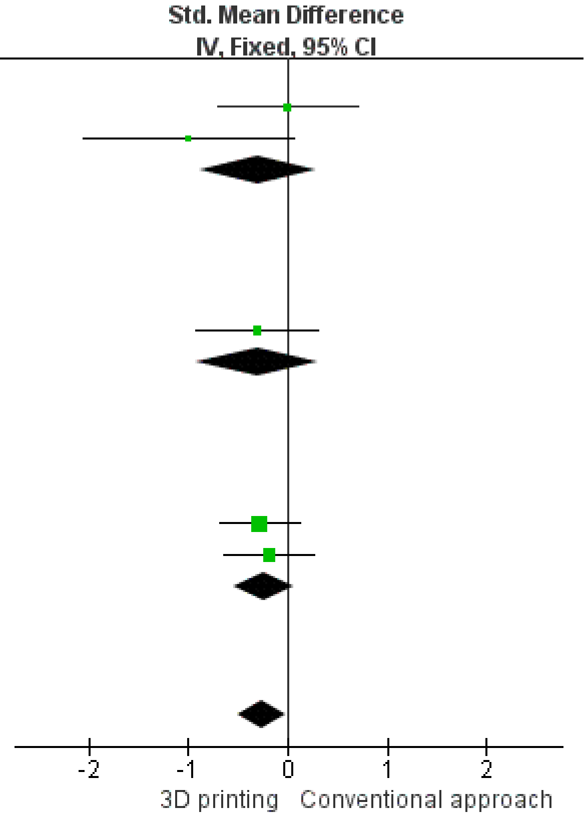

Figure e. The forest plot of subgroup analysis for visual analogue scale (VAS). CI, confidence interval; IV, inverse variance; SD, standard deviation.

Study or Subgroup	3D printing Mean	3D printing SD	3D printing Total	Conventional approach Mean	Conventional approach SD	Conventional approach Total	Weight	Std. Mean Difference IV, Random, 95% CI
10.1.1 Upper limb								
Chen et al, 2019	75.7	15.5	23	74.8	16.6	25	7.6%	0.06 [-0.51, 0.62]
Kong et al, 2020	23.8	8.1	16	24.5	7	16	5.1%	-0.09 [-0.78, 0.60]
Shuang et al, 2016	85	9	6	79	13	7	2.0%	0.49 [-0.62, 1.61]
Yin et al, 2020	84.4	7.8	8	72.5	10	8	2.0%	1.25 [0.15, 2.36]
Zheng et al, 2018 (3)	85.2	9.6	43	83.1	10	48	14.4%	0.21 [-0.20, 0.62]
Subtotal (95% CI)			**96**			**104**	**31.1%**	**0.22 [-0.10, 0.54]**
Heterogeneity: Tau² = 0.02; Chi² = 4.71, df = 4 (P = 0.32); I² = 15%								
Test for overall effect: Z = 1.36 (P = 0.18)								
10.1.2 Spine								
Feng et al, 2020	12.83	1.17	6	11.83	0.98	6	1.7%	0.86 [-0.35, 2.06]
Wei et al, 2020	16.35	0.93	20	15.35	1.81	20	6.0%	0.68 [0.04, 1.32]
Subtotal (95% CI)			**26**			**26**	**7.7%**	**0.72 [0.15, 1.28]**
Heterogeneity: Tau² = 0.00; Chi² = 0.06, df = 1 (P = 0.80); I² = 0%								
Test for overall effect: Z = 2.50 (P = 0.01)								
10.1.3 Lower limb								
Hasan et al, 2020	33	9.2	35	30	8.9	34	10.8%	0.33 [-0.15, 0.80]
Sun et al, 2020	87.4	8.2	40	86.3	7.6	40	12.7%	0.14 [-0.30, 0.58]
Wu et al, 2020	95.2	2.5	18	94.9	2.2	16	5.4%	0.12 [-0.55, 0.80]
Zhang et al, 2016	82.9	16.8	20	72.8	10.9	20	6.0%	0.70 [0.06, 1.34]
Zheng et al, 2018	87.4	8.7	45	84.7	9	48	14.6%	0.30 [-0.11, 0.71]
Zheng et al, 2018 (2)	87.6	7.6	35	85.8	9	40	11.8%	0.21 [-0.24, 0.67]
Subtotal (95% CI)			**193**			**198**	**61.3%**	**0.28 [0.08, 0.48]**
Heterogeneity: Tau² = 0.00; Chi² = 2.39, df = 5 (P = 0.79); I² = 0%								
Test for overall effect: Z = 2.73 (P = 0.006)								
Total (95% CI)			**315**			**328**	**100.0%**	**0.29 [0.13, 0.45]**
Heterogeneity: Tau² = 0.00; Chi² = 9.71, df = 12 (P = 0.64); I² = 0%								
Test for overall effect: Z = 3.64 (P = 0.0003)								
Test for subgroup differences: Chi² = 2.39, df = 2 (P = 0.30), I² = 16.5%								

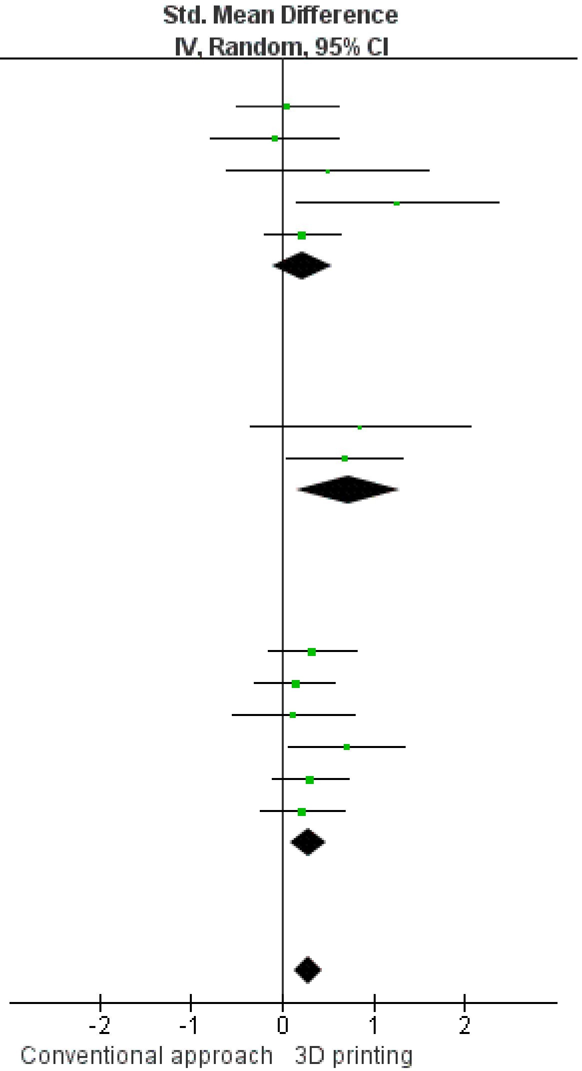

Figure f. The forest plot of subgroup analysis for functional score in upper limb, spine, and lower limb. CI, confidence interval; IV, inverse variance; SD, standard deviation.

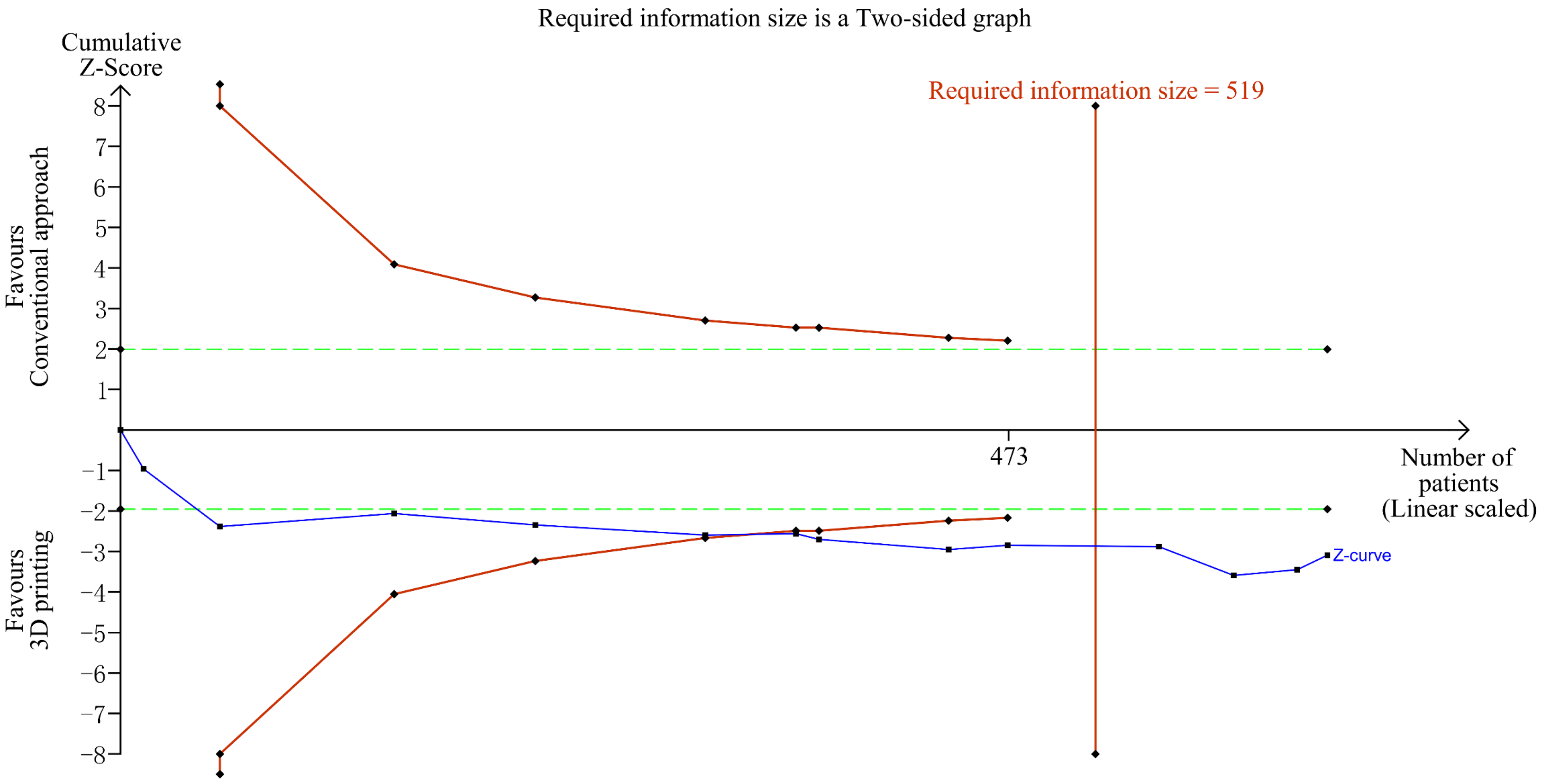

Figure g. Trial sequential analysis for functional score. Trial sequential analysis (TSA) of 13 trials (black squares on the blue line) was shown to explore the effects of 3D printing on the follow-up functional scores compared to the conventional approach group. TSA showed the line of cumulative Z-curve (blue) crossed the conventional boundary (green) and trial sequential monitoring boundary (red curve), favouring 3D printing, as well as the required information size (red vertical line). The number of patients (n = 643) exceeded the required information size (n = 519).

References

1. **Shuang F, Hu W, Shao Y, Li H, Zou H.** Treatment of Intercondylar Humeral Fractures With 3D-Printed Osteosynthesis Plates. *Medicine (Baltimore)*. 2016;95: e2461.

2. **Zheng W, Chen C, Zhang C, Tao Z, Cai L.** The Feasibility of 3D Printing Technology on the Treatment of Pilon Fracture and Its Effect on Doctor-Patient Communication. *Biomed Res Int*. 2018;8054698.

3. **Chen C, Cai L, Zheng W, Wang J, Guo X, Chen H.** The efficacy of using 3D printing models in the treatment of fractures: a randomised clinical trial. *BMC Musculoskelet Disord*. 2019;20(65).

4. **Huang JH, Liao H, Tan XY, et al.** Surgical treatment for both-column acetabular fractures using pre- operative virtual simulation and three-dimensional printing techniques. *Chin Med J (Engl)*. 2020;133:395-401.

5. **You W, Liu LJ, Chen HX, et al.** Application of 3D printing technology on the treatment of complex proximal humeral fractures (Neer3-part and 4-part) in old people. *Orthop Traumatol Surg Res.* 2016;102:897-903.

6. **Kong L, Yang G, Yu J, et al.** Surgical treatment of intra-articular distal radius fractures with the assistance of three-dimensional printing technique. *Medicine (Baltimore)*. 2020;99:e19259.

7. **Feng S, Lin J, Su N, Meng H, Yang Y, Fei Q.** 3-Dimensional printing templates guiding versus free hand technique for cervical lateral mass screw fixation: A prospective study. *J Clin Neurosci*. 2020;78:252-258.

8. **Du H, Tian XX, Li TS, et al.** Use of patient-specific templates in hip resurfacing arthroplasty: experience from sixteen cases. *Int Orthop.* 2013;37:777-782.

9. **Merc M, Drstvensek I, Vogrin M, Brajlih T, Recnik G.** A multi-level rapid prototyping drill guide template reduces the perforation risk of pedicle screw placement in the lumbar and sacral spine. *Arch Orthop Trauma Surg*. 2013;**133**: 893-899.

10. **Zhang YZ, Lu S, Zhang HQ, et al.** Alignment of the lower extremity mechanical axis by computer- aided design and application in total knee arthroplasty. *Int J Comput Assist Radiol Surg*. 2016;11:1881-1890.

11. **Hu X, Zhong M, Lou Y, et al.** Clinical application of individualized 3D-printed navigation template to children with cubitus varus deformity. *J Orthop Surg Res.* 2020;15:111.

12. **Sun ML, Zhang Y, Peng Y, Fu DJ, Fan HQ, He R.** Accuracy of a Novel 3D-Printed Patient-Specific Intramedullary Guide to Control Femoral Component Rotation in Total Knee Arthroplasty. *Orthopaedic Surg*. 2020;12(2):429-441.

13. **Wu Q, Yu T, Lei B, Huang W, Huang R.** A New Individualized Three- Dimensional Printed Template for Lateral Ankle Ligament Reconstruction. *Med Sci*

Monit. 2020;26: e922925.

14. **Yin HW, Feng JT, Yu BF, Shen YD, Gu YD, Xu WD.** 3D printing-assisted percutaneous fixation makes the surgery for scaphoid nonunion more accurate and less invasive. *J Orthop Translat.* 2020;24:138-143.

15. **Zhang M, Li J, Fang T, et al.** Evaluation of a Three-Dimensional Printed Guide and a Polyoxymethylene Thermoplastic Regulator for Percutaneous Pedicle Screw Fixation in Patients with Thoracolumbar Fracture. *Med Sci Monit.* 2020;26: e920578.

16. **Hasan S, van Hamersveld KT, Marang-van de Mheen PJ, Kaptein BL, Nelissen RGHH, Toksvig-Larsen S.** Migration of a novel 3D-printed cementless versus a cemented total knee arthroplasty: two-year results of a randomized controlled trial using radiostereometric analysis. *Bone Joint J.* 2020;102-B(8):1016-1024.

17. **Wei F, Xu N, Li Z, et al.** A prospective randomized cohort study on 3D-printed artificial vertebral body in single-level anterior cervical corpectomy for cervical spondylotic myelopathy. *Ann Transl Med.* 2020;8(17):1070.

18. **Yang L, Shang XW, Fan JN, et al.** Application of 3D Printing in the Surgical Planning of Trimalleolar Fracture and Doctor-Patient Communication. *Biomed Res Int.* 2016, 2482086.

19. **Maini L, Verma T, Sharma A, Sharma A, Mishra A, Jha S.** Evaluation of accuracy of virtual surgical planning for patient-specific pre-contoured plate in acetabular fracture fixation. *Arch Orthop Trauma Surg.* 2018;138(4): 495-504.

20. **Zheng W, Tao Z, Lou Y, et al.** Comparison of the Conventional Surgery and the Surgery Assisted by 3d Printing Technology in the Treatment of Calcaneal Fractures. *J Invest Surg*. 2018;31(6):557-567.

21. **Zheng W, Su J, Cai L, et al.** Application of 3D-printing technology in the treatment of humeral intercondylar fractures. *Orthop Traumatol Surg Res*. 2018;104: 83-88.